

# Near-Field Channel Estimation for XL-RIS Assisted Multi-User XL-MIMO Systems: Hybrid Beamforming Architectures

Jeongjae Lee, *Student Member, IEEE*, Hyeonjin Chung, *Student Member, IEEE*, Yunseong Cho, *Member, IEEE*, Sunwoo Kim, *Senior Member, IEEE* and Songnam Hong, *Member, IEEE*

**Abstract**—Channel estimation is one of the key challenges for the deployment of extremely large-scale reconfigurable intelligent surface (XL-RIS) assisted multiple-input multiple-output (MIMO) systems. In this paper, we study the channel estimation problem for XL-RIS assisted multi-user XL-MIMO systems with hybrid beamforming structures. For this system, we propose an *unified* channel estimation method that yields a notable estimation accuracy in the near-field BS-RIS and near-field RIS-User channels (in short, near-near field channels), far-near field channels, and far-far field channels. Our key idea is that the effective (or cascaded) channels to be estimated can be each factorized as the product of low-rank matrices (i.e., the product of the common (or user-independent) matrix and the user-specific coefficient matrix). The common matrix whose columns are the basis of the column space of the BS-RIS channel matrix is efficiently estimated via a *collaborative* low-rank approximation (CLRA). Leveraging the hybrid beamforming structures, we develop an efficient iterative algorithm that jointly optimizes the user-specific coefficient matrices. Via experiments and complexity analysis, we verify the effectiveness of the proposed channel estimation method (named CLRA-JO) in the aforementioned three classes of wireless channels.

**Index Terms**—Reconfigurable intelligent surface (RIS), XL-MIMO, channel estimation, hybrid beamforming, low-rank approximation.

## I. INTRODUCTION

Reconfigurable intelligent surface (RIS) is a promising technology for robust millimeter-wave (mmWave) and terahertz (THz) multiple-input multiple-output (MIMO) systems [1]–[3]. A RIS consists of a uniform array with a large number of reflective elements, each of which can control the phase and reflection angle of the incident signal so that the received power of the intended signal is enhanced [4]. The potential advantages of the RIS open up new research opportunities such as reflect beamforming design [5]–[8] and RIS-aided localization and sensing [9]–[11]. Nonetheless, the accuracy

of a channel estimation plays a crucial role in implementing numerous RIS-assisted applications [11].

There have been numerous works on the design of an efficient channel estimation method in RIS-aided mmWave MIMO systems. Herein, the channel responses between the base station (BS) and the RIS (in short, the BS-RIS channel) and between the RIS and the users (in short, the RIS-User channels) are assumed as *far-field* channels. Accordingly, both BS and RIS will experience *planar-wavefront*. The primary goal of the existing works is to estimate the channel accurately while having an affordable training overhead. Toward this, the key idea is to exploit the *sparsity* of mmWave channels, which comes from the fact that there exists a smaller number of signal paths in the BS-RIS channel. The de-facto channel estimation method to harness the sparsity is based on compressed sensing (CS). Specifically, the angle-of-departures (AoDs) and the angle-of-arrivals (AoAs) of sparse signal paths are estimated via CS, thus requiring less training overhead. In [12], the popular orthogonal matching pursuit (OMP) was used as a low-complexity CS method. An enhanced CS-based method was developed in [13], by exploiting the subspace estimation and the so-called scaling property of the RIS-User channels. Unfortunately, the CS-based methods suffer from the inevitable *grid-mismatch* problem [14] since a dictionary matrix is constructed by quantizing steering vectors at a specific resolution. Having an affordable computational complexity (i.e., the quantization levels), the CS-based methods can result in a severe error-floor problem due to the quantization errors.

Besides the CS-based channel estimation methods, approximate message passing (AMP)-based methods were developed in [15], [16], which is based on the parallel factor decomposition to unfold the so-called effective (or cascaded) channels to be estimated. In [15], alternating least squares (ALS) and vector AMP (VAMP) were presented as efficient iterative algorithms. Also, in [16], unitary AMP (UAMP)-based method was presented, which is more computationally efficient than the ALS- and VAMP-based methods. Noticeably, the AMP-based methods are only applicable in larger systems such that the number of users (denoted by  $K$ ) is not less than the number of reflective elements (denoted by  $N$ ) in the RIS. In the example of  $N = 128$ , the AMP-based methods can be used at least when  $K \geq 128$ . This can limit the applicability of the AMP-based channel estimation methods in various RIS-aided applications.

In future communication systems (e.g., 6G), the number

J. Lee, H. Chung, S. Kim, and S. Hong are with the Department of Electronic Engineering, Hanyang University, Seoul, Korea (e-mail: {lyjcje7466, hyeonjingo, remero, snhong}@hanyang.ac.kr).

Y. Cho is with Samsung Research America, Plano, Texas, USA (e-mail: yscho@utexas.edu).

This work was supported in part by the Technology Innovation Program (1415178807, Development of Industrial Intelligent Technology for Manufacturing, Process, and Logistics) funded By the Ministry of Trade, Industry & Energy(MOTIE, Korea) and in part by the Institute of Information & communications Technology Planning & Evaluation (IITP) under the artificial intelligence semiconductor support program to nurture the best talents (IITP-(2024)-RS-2023-00253914) grant funded by the Korea government(MSIT).

of reflective elements in the RIS tends to be extremely large (XL) to further enhance the beamforming gain [17], [18]. This will lead to a larger Rayleigh distance (RD), which is the boundary between the near- and far-field channels. For example, when the RIS is equipped with 256 half-wavelength spacing elements at operating 100GHz, the RD becomes almost 100m [19]. In the 6G systems, thus, the near-field effect becomes non-negligible and accordingly, the RIS will experience *spherical-wavefront* rather than planar-wavefront (see Fig. 2(b)). Recall that the aforementioned channel estimation methods based on the planar-wavefront heavily rely on the channel sparsity in the angular domain. Due to the near-field effect in the spherical-wavefront, however, the channel sparsity in the angular domain is no longer applicable. It is necessary to develop an efficient channel estimation method for near-field XL-RIS assisted MIMO systems. Assuming that the RIS-User channels are near-field, the channel estimation problem was formulated as the CS problem by means of the polar-domain sparsity [17], [20]. Based on this, a single measurement vector (SMV)-based OMP algorithm was presented as an efficient channel estimation method. As expected, this method suffers from the grid-mismatch problem.

In the above works, it is assumed that BS is equipped with fully-digital structures. However, when the BS is equipped with a massive or extremely large number of antennas, the use of a large number of radio frequency (RF) chains (i.e., one for each antenna component) significantly increases the cost and the energy consumption [21], [22]. A promising solution to these problems lies in the concept of hybrid beamforming structures, which takes the combination of analog beamforming in the RF domain, together with digital beamforming in the baseband connected to the RF chains [22]. Therefore, XL-RIS assisted XL-MIMO systems with hybrid beamforming structures can be considered as a promising energy-efficient technology [23]–[25]. Recently in [26]–[29], the channel estimation method for RIS-aided mmWave MIMO systems with hybrid beamforming structures was investigated, in which all channels are assumed as *far-field* channels. In [26], [27], the grid-mismatch problem was alleviated via atomic norm minimization (ANM). However, the ANM-based methods are impractical due to their expensive computational complexities. In [28], [29], the channel estimation problem was formulated as a low-rank matrix completion (LRMC) and then solved via fast alternating least squares (FALS) [30]. Also, it was shown that the LRMC-based method can outperform the CS-based methods by avoiding the grid-mismatch problem [28], [29]. Nevertheless, this method suffers from the *noisy-sample* problem, which is inevitable due to the use of matrix completion with *noisy* observations. Specifically, the sampled noisy elements cannot be updated via the proposed matrix completion method in [28], [29] and thus, the estimation accuracy is saturated as the pilot overhead (i.e., the number of sampled elements) grows. In [31], [32], the XL-RIS assisted MU-MIMO systems with hybrid beamforming structures, which is the most related to our system model, was investigated, where the BS-RIS and the RIS-User channels are assumed as *far- and near-field* channels, respectively. In [31], the two-phase channel estimation protocol was proposed to improve the

efficiency of training overhead. Based on this framework, a 3-dimensional multiple measurement vector (MMV) look-ahead OMP (3D-MLAOMP) was developed as an efficient channel estimation method. This method still suffers from the grid-mismatch problem and requires some impractical assumptions such as the number of spatial paths and the angle of line-of-sight (LoS) path being given a priori. In [32], a fast-sparse-Bayesian-learning (FSBL)-based channel estimation method was proposed by focusing on the limited visual region (VR) of the channel between the RIS and each user in XL-RIS systems. This method is impractical due to the expensive computational complexity since a super-resolution (SR) algorithm is used to estimate the common AoD at the BS and its complexity is too expensive. Thus, it is an open problem to develop an efficient channel estimation method for XL-RIS assisted XL-MIMO systems.

Motivated by the above, in this paper, we study the channel estimation problem for XL-RIS assisted multi-user XL-MIMO systems with hybrid beamforming structures. Noticeably, it is assumed that both the BS and the RIS are equipped with extremely large-scale antenna array (ELAA). Accordingly, we consider the following categories of wireless channels: i) Far-field BS-RIS and far-field RIS-User channels (i.e., *far-far* field channel); ii) Far-field BS-RIS and near-field RIS-User channels (i.e., *far-near* field channel); iii) Near-field BS-RIS and near-field RIS-User channels (i.e., *near-near* field channel). Beyond the existing works in [31], [32], we for the first time investigate the channel estimation method for near-near field channels. In addition, as an extension of the existing works, the proposed channel estimation method can be performed when each user is equipped with a multiple antenna. The major contributions of this paper are summarized as follows.

- We develop an *unified* channel estimation method that can be performed on *near- and far-field* uniform planar array (UPA) MIMO channels without any modification. Furthermore, we present a two-phase communication protocol suitable for the proposed channel estimation method, by harnessing the fact that BS-RIS and RIS-User channels have different channel coherence times. This can considerably reduce the training overhead.
- In mmWave and THz communication systems, there exists a small number of signal paths in the BS-RIS channel. Thus, the effective (or cascaded) channels to be estimated (denoted by  $\{\mathbf{H}_{[\text{eff},k]} : k \in [K]\}$ ) have lower-dimensional *common* column space regardless of the aforementioned channel categories. Leveraging this, each effective channel can be categorized as the product of low-rank matrices, i.e.,  $\mathbf{H}_{[\text{eff},k]} = \mathbf{S}_{\text{col}} \mathbf{T}_k$ , where  $\mathbf{S}_{\text{col}}$  contains the basis of the common column space and  $\mathbf{T}_k$  denotes a user-specific coefficient matrix.
- Based on the above low-rank factorization, the proposed channel estimation method consists of two parts. In the first part, we estimate the dimension of the column space (i.e., the size of the matrix  $\mathbf{S}_{\text{col}}$ ) using the minimum description length (MDL) criterion and then estimate  $\mathbf{S}_{\text{col}}$  by means of a collaborative low-rank approximation

(CLRA). Via theoretical analysis, it is proved that the accuracy of the estimated  $\mathbf{S}_{\text{col}}$  is inversely proportional to the product of the pilot overhead and the number of users  $K$ . To achieve a target accuracy level, the pilot overhead can be reduced as the pilot overhead grows, namely, a multi-user gain can be attained.

- In the second part, we propose an efficient iterative algorithm to *jointly* optimize the user-specific coefficient matrices  $\{\mathbf{T}_k : k \in [K]\}$ . Herein, the joint optimization is formulated using the fact that  $\mathbf{H}_{[\text{eff},k]} = \mathbf{D}_k \mathbf{H}_{[\text{eff},1]}$ ,  $\forall k \in [K]$ , with some diagonal matrix  $\mathbf{D}_k$ . We show that this joint optimization can significantly enhance the signal-to-noise ratio (SNR) gain compared with the standard *individual* least-square (LS) estimations. Also, the convergence of the proposed iterative algorithm is theoretically proved.
- The proposed channel estimation method is referred to as Collaborative Low-Rank Approximation and Joint Optimization (CLRA-JO). Via experiments and complexity analysis, we verify the effectiveness of the proposed CLRA-JO. In various channel environments, the proposed method can yield better estimation accuracy than the state-of-the-art CS-based methods while having lower training overhead (e.g., about 80% reduction of the training overhead).

The remaining part of this paper is organized as follows. In Section II, we define the channel and signal models for XL-RIS assisted multi-user XL-MIMO systems with hybrid beamforming structures. Section III introduces the channel estimation protocol and the frame structures. In Section IV, we describe the proposed channel estimation method, named CLRA-JO. Section V provides simulation results and Section VI concludes the paper.

*Notations.* Let  $[N_1 : N_2] \triangleq \{N_1, N_1 + 1, \dots, N_2\}$  for any positive integers  $N_1$  and  $N_2$  with  $N_1 < N_2$ . When  $N_1 = 1$ , it is further simplified as  $[N_2] \triangleq \{1, 2, \dots, N_2\}$ . We use  $\mathbf{x}$  and  $\mathbf{A}$  to denote a column vector and matrix, respectively. Also,  $\mathbf{A}^\dagger$  denotes the Moore-Penrose inverse and  $\otimes$  denotes the Kronecker product. Given a  $M \times N$  matrix  $\mathbf{A}$ , let  $\mathbf{A}(i, :)$  and  $\mathbf{A}(:, j)$  denote the  $i$ -th row and  $j$ -th column of  $\mathbf{A}$ , respectively. Also, given the index subsets  $\mathcal{I}_{\text{row}} \subseteq [M]$  and  $\mathcal{I}_{\text{col}} \subseteq [N]$ , we let  $\mathbf{A}(\mathcal{I}_{\text{row}}, :)$  and  $\mathbf{A}(:, \mathcal{I}_{\text{col}})$  denote the submatrices of  $\mathbf{A}$  by only taking the rows and columns whose indices are belong to  $\mathcal{I}_{\text{row}}$  and  $\mathcal{I}_{\text{col}}$ , respectively. Given a vector  $\mathbf{v}$ ,  $\text{diag}(\mathbf{v})$  denotes a diagonal matrix whose  $\ell$ -th diagonal element is equal to the  $\ell$ -th element of  $\mathbf{v}$ . We let  $\mathbf{I}$  and  $\mathbf{0}$  denote the identity and all-zero matrices, respectively, where the sizes of these matrices are easily obtained from the context.

## II. SYSTEM MODEL

We consider an uplink time-division-duplexing (TDD) multi-user multiple-input multiple-output (MU-MIMO) system. In this system, a reconfigurable intelligent surface (RIS) with  $N$  reflective elements assists the communication between the base station (BS) with  $M$  antennas and the  $K$  users each having  $L$  antennas (see Fig. 1). Noticeably, it is assumed that

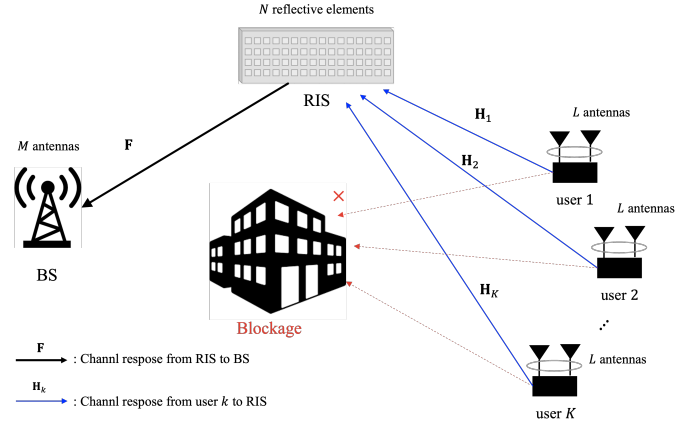


Fig. 1. A RIS-aided MU-MIMO system consisting of the BS with  $M$  antennas, the RIS with  $N$  reflective elements, and the  $K$  users with  $L$  antennas.

both the BS and the RIS are equipped with extremely large-scale antenna array (ELAA). For the sake of lower complexity, cost and power consumption [22], [33], the BS is assumed to use the hybrid beamforming with a limited number of radio frequency (RF) chains, where  $N_{\text{RF}} \leq M$  denotes the number of RF chains at the BS. As considered in the related works [28], [29], [31], [32], it is assumed that the direct channels between the BS and the  $K$  users are blocked (see Fig. 1). The channel responses from the  $k$ -th user to the RIS and from the RIS to the BS are respectively denoted as  $\mathbf{H}_k \in \mathbb{C}^{N \times L}$  and  $\mathbf{F} \in \mathbb{C}^{M \times N}$ . The reflection vector in the RIS is denoted as  $\mathbf{v} = [v_1, v_2, \dots, v_N]^H$  with  $v_n = e^{j\vartheta_n}$ , where  $\vartheta_n \in [0, 2\pi)$  is the phase shift of the  $n$ -th reflective element. We note that the proposed channel estimation method in Section IV can be applied to both continuous and discrete phase shifting RISs. Taking this into account, the total channel response from the  $k$ -th user to the BS is defined as

$$\mathbf{F} \text{diag}(\mathbf{v}) \mathbf{H}_k = \mathbf{H}_{[\text{eff},k]} (\mathbf{I} \otimes \mathbf{v}), \quad (1)$$

where the effective (or cascaded) channel is defined as

$$\mathbf{H}_{[\text{eff},k]} \triangleq [\mathbf{H}_{[\text{eff},k,1]} \quad \dots \quad \mathbf{H}_{[\text{eff},k,L]}] \in \mathbb{C}^{M \times NL}, \quad (2)$$

and where

$$\mathbf{H}_{[\text{eff},k,\ell]} = \mathbf{F} \text{diag}(\mathbf{H}_k(:, \ell)) \in \mathbb{C}^{M \times N}. \quad (3)$$

*Remark 1:* We emphasize that the definition of our effective channel in (2) is different from that in [26], [27]. In the latter, an effective channel is defined as the Kronecker product of the BS-RIS and RIS-User channels. This expression is not suitable for the joint optimization of the reflection vector and the hybrid beamforming due to its large dimension. In contrast, the proposed effective channel has a more compact form, thereby being more adequate for the joint optimization, as shown in [34]–[37]. Motivated by this, we in this paper aim at developing an efficient method to estimate the effective channels  $\{\mathbf{H}_{[\text{eff},k]} : k \in [K]\}$ . ■

In the remaining part of this section, we will describe the specific channel models for  $\{\mathbf{H}_k : k \in [K]\}$  and  $\mathbf{F}$ . We first provide the useful definition:

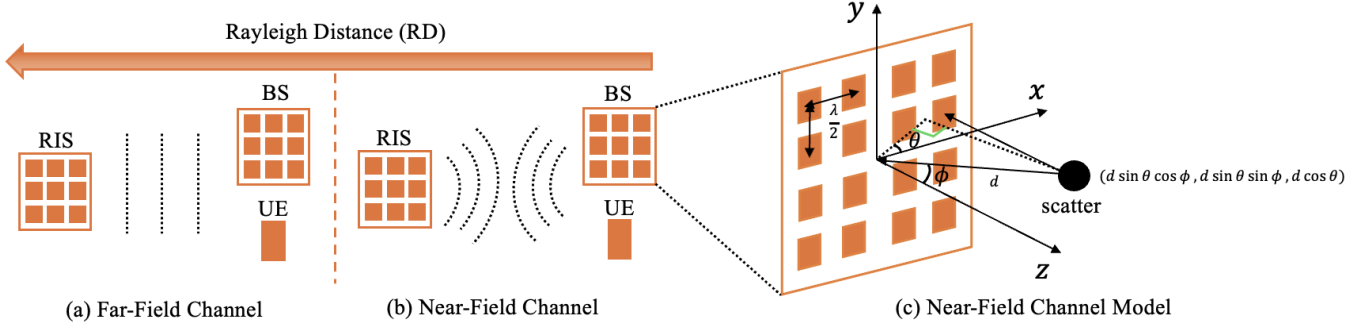


Fig. 2. The categories of wireless channels  $\{\mathbf{H}_k : k \in [K]\}$  and  $\mathbf{F}$ . (a) The far-field region, where the planar-wavefront is assumed. (b) The near-field region, where the spherical-wavefront is assumed. (c) The near-field channel model for UPA communication system based on 3D-coordinate.

*Definition 1:* Given an array size  $X = E_h \times E_v$ , a distance between the scatter and the center of array  $d$ , an elevation angle  $\theta \in [0, 2\pi)$  and azimuth angle  $\phi \in [0, \pi)$ , we define a *near-field* array response vector [38] (see Fig. 2 (c)):

$$\mathbf{b}_X(d, \theta, \phi) \triangleq \sqrt{\frac{1}{X}} \left[ e^{-j \frac{2\pi}{\lambda} \Delta d(1,1)}, \dots, e^{-j \frac{2\pi}{\lambda} \Delta d(E_h, E_v)} \right]^\top, \quad (4)$$

where for  $e_h \in [E_h], e_v \in [E_v]$ ,

$$\begin{aligned} \Delta d(e_h, e_v) \approx & -\sin \theta \cos \phi x_{e_h} - \sin \theta \sin \phi y_{e_v} \\ & + \frac{1 - \sin^2 \theta \cos^2 \phi}{2d} x_{e_h}^2 + \frac{1 - \sin^2 \theta \sin^2 \phi}{2d} y_{e_v}^2 \\ & - \frac{\sin^2 \theta \cos \phi \sin \phi}{d} x_{e_h} y_{e_v}, \end{aligned} \quad (5)$$

where  $x_{e_h} = \frac{\lambda}{2}(e_h - (E_h + 1)/2)$  and  $y_{e_v} = \frac{\lambda}{2}(e_v - (E_v + 1)/2)$ . When  $d$  is sufficiently large, the last three terms in (5) can be negligible. In this case, the array response vector  $\mathbf{b}_X(d, \theta, \phi)$  is simplified as

$$\mathbf{a}_X(\theta, \phi) \triangleq \sqrt{\frac{1}{X}} \left[ 1, \dots, e^{j\pi(e_h \sin \theta \cos \phi + e_v \sin \theta \sin \phi)}, \dots, e^{j\pi((E_h-1) \sin \theta \cos \phi + (E_v-1) \sin \theta \sin \phi)} \right]^\top. \quad (6)$$

Note that this is equivalent to the conventional *far-field* UPA array response vector. ■

In Section II-A and Section II-B, we describe the specific wireless channel models according to the distances between the BS and the RIS, and between the RIS and the  $K$  users. Throughout the paper, we let  $z_f$  and  $z_{h_k}$  denote the physical distances between the BS and the RIS, and between the RIS and the user  $k$ , respectively.

#### A. RIS-User Channels

We describe the RIS-User channels (i.e.,  $\mathbf{H}_k$  for  $k \in [K]$ ). To categorize these channels, we define the Rayleigh distance (RD), given by [17]:

$$Z_{\text{RD}} = \frac{2D_{\text{RIS}}^2}{\lambda}, \quad (7)$$

where  $\lambda$  is the wavelength of EM wave and  $D_{\text{RIS}}$  is the RIS aperture (i.e.,  $D_{\text{RIS}} = (\lambda/2)N$ ). As depicted in Fig. 2, each  $\mathbf{H}_k$  can be classified into the near- and far-field channels.

Specifically, for  $z_{h_k} < Z_{\text{RD}}$ ,  $\mathbf{H}_k$  is considered as the near-field channel and the wavefronts are approximated as spherical waves (see Fig. 2 (b)). Otherwise, it is considered as the far-field channel and the wavefronts are approximated as planar waves (see Fig. 2 (a)). Using the array response vectors in Definition 1,  $\{\mathbf{H}_k : k \in [K]\}$  can be described as follows:

- Near-field channel ( $z_{h_k} \leq Z_{\text{RD}}$ ):

$$\begin{aligned} \mathbf{H}_k = & \sum_{i=1}^{N_{h_k}} \alpha_{h_k}^i \mathbf{b}_N \left( d_{[h_k, r]}^i, \theta_{[h_k, r]}^i, \phi_{[h_k, r]}^i \right) \\ & \times \mathbf{a}_L^H \left( \theta_{[h_k, t]}^i, \phi_{[h_k, t]}^i \right), \end{aligned}$$

- Far-field channel ( $z_{h_k} > Z_{\text{RD}}$ )

$$\mathbf{H}_k = \sum_{i=1}^{N_{h_k}} \alpha_{h_k}^i \mathbf{a}_N \left( \theta_{[h_k, r]}^i, \phi_{[h_k, r]}^i \right) \mathbf{a}_L^H \left( \theta_{[h_k, t]}^i, \phi_{[h_k, t]}^i \right),$$

where  $N_{h_k}$  is the number of spatial paths,  $d_{[h_k, r]}^i$  is the distance between  $i$ -th scatter and the RIS,  $\theta_{[h_k, r]}^i$  (resp.  $\theta_{[h_k, t]}^i$ ) and  $\phi_{[h_k, r]}^i$  (resp.  $\phi_{[h_k, t]}^i$ ) are the elevation and azimuth angle of arrival (resp. departure) for the RIS (resp. user  $k$ ), respectively.

#### B. BS-RIS Channel

We describe the BS-RIS channel (i.e.,  $\mathbf{F}$ ). To classify this channel, we define the MIMO Rayleigh distance (MIMO-RD), given by [20]:

$$Z_{\text{MRD}} \triangleq \frac{2(D_{\text{RIS}} + D_{\text{BS}})^2}{\lambda}, \quad (8)$$

where  $D_{\text{RIS}} = (\lambda/2)N$  and  $D_{\text{BS}} = (\lambda/2)M$  denote the antenna apertures of the RIS and the BS, respectively. Using the array response vectors in Definition 1,  $\mathbf{F}$  can be described as follows:

- Near-field channel ( $z_f \leq Z_{\text{MRD}}$ ):

$$\begin{aligned} \mathbf{F} = & \sum_{i=1}^{N_f} \alpha_f^i \mathbf{b}_M \left( d_{[f, r]}^i, \theta_{[f, r]}^i, \phi_{[f, r]}^i \right) \\ & \times \mathbf{b}_N^H \left( d_{[f, t]}^i, \theta_{[f, t]}^i, \phi_{[f, t]}^i \right), \end{aligned}$$

- Far-field channel ( $z_f > Z_{\text{MRD}}$ ):

$$\mathbf{F} = \sum_{i=1}^{N_f} \alpha_f^i \mathbf{a}_M \left( \theta_{[f,r]}^i, \phi_{[f,r]}^i \right) \mathbf{a}_N^H \left( \theta_{[f,t]}^i, \phi_{[f,t]}^i \right),$$

where  $N_f$  is the number of spatial paths,  $d_{[f,r]}^i$  (resp.  $d_{[f,t]}^i$ ) are distance between  $i$ -th scatter and the BS (resp. the RIS),  $\theta_{[f,r]}^i$  (resp.  $\theta_{[f,t]}^i$ ) and  $\phi_{[f,r]}^i$  (resp.  $\phi_{[f,t]}^i$ ) are elevation and azimuth angle of arrival (resp. departure) for the BS (resp. the RIS), respectively.

For the first time, we propose an *unified* channel estimation method in Section IV, which can perform in the following categories of wireless channels:

- Far-far field channels: Both  $\mathbf{F}$  and  $\{\mathbf{H}_k : k \in [K]\}$  are all far-field channels.
- Far-near field channels:  $\mathbf{F}$  is a far-field channel and  $\{\mathbf{H}_k : k \in [K]\}$  are all near-field channels.
- Near-near field channels: Both  $\mathbf{F}$  and  $\{\mathbf{H}_k : k \in [K]\}$  are all near-field channels.

On the other hand, in the existing compressed sensing (CS)-based methods [13], [31], a dictionary should be designed by taking into account the characteristics of the near- and far-field channels.

### III. CHANNEL ESTIMATION PROTOCOL

The channel estimation protocol performs with  $J$  subframes, each of which consists of  $T$  symbols (or time slots) with  $T \geq KL$ . Accordingly, it requires the total  $JT$  symbols, where the hyperparameter  $J$  can control the tradeoff between the estimation accuracy and the training overhead. Throughout the paper,  $J$  is referred to as the training overhead. In the proposed protocol, the RIS reflection vector  $\mathbf{v}_j = [v_{[j,1]}, v_{[j,2]}, \dots, v_{[j,N]}]^T$  and the  $M \times N_{\text{RF}}$  RF combining matrix  $\mathbf{C}_j$  are unchanged within each subframe  $j \in [J]$ , but they can be changed across the subframes. Their specific constructions will be provided in Section IV.

During the  $J$  subframes, our channel estimation protocol proceeds as follows. At every subframe  $j \in [J]$ , each user  $k \in [K]$  transmits its orthogonal pilot sequence of the length  $T$  to the BS, denoted by  $\mathbf{X}_{[j,k]} \in \mathbb{C}^{L \times T}$ , such that

$$\mathbf{X}_{[j,k]} \mathbf{X}_{[j,k]}^H = PT \times \mathbf{I}, \quad (9)$$

where  $PT$  is the energy constraint,  $P$  is the transmit power of each user and antenna, and  $\mathbf{X}_{[j,k]} \mathbf{X}_{[j,k']}^H = \mathbf{0}$  if  $k \neq k'$ . This construction is always possible due to the choice of  $T \geq KL$ . Note that each user  $k$  sends the  $i$ -th row of  $\mathbf{X}_{[j,k]}$  through the  $i$ -th transmit antenna during the  $T$  time slots. For each subframe  $j \in [J]$ , the BS then observes the  $N_{\text{RF}} \times T$  matrix, given by

$$\mathbf{Y}_j = \mathbf{C}_j^H \left( \sum_{k=1}^K (\mathbf{F} \text{diag}(\mathbf{v}_j) \mathbf{H}_k) \mathbf{X}_{[j,k]} + \mathbf{U}_j \right), \quad (10)$$

where  $\mathbf{U}_j$  is the noise matrix whose elements follow independently identically circularly symmetric complex Gaussian distribution with mean zero and variance  $\sigma^2$ . Leveraging the

orthogonality of the pilot sequences, we can derive the user-specific observation:

$$\begin{aligned} \mathbf{Z}_{[j,k]} &= \frac{1}{PT} \mathbf{Y}_j \mathbf{X}_{[j,k]}^H \in \mathbb{C}^{N_{\text{RF}} \times L} \\ &= \mathbf{C}_j^H (\mathbf{F} \text{diag}(\mathbf{v}_j) \mathbf{H}_k + \mathbf{N}_{[j,k]}), \end{aligned} \quad (11)$$

for  $k \in [K]$ , where  $\mathbf{N}_{[j,k]} \triangleq \frac{1}{PT} \mathbf{U}_j \mathbf{X}_{[j,k]}^H$ . Stacking the  $K$  user-specific observations, we define:

$$\begin{aligned} \mathbf{Z}_j &\triangleq [\mathbf{Z}_{[j,1]} \quad \dots \quad \mathbf{Z}_{[j,K]}] \\ &= \mathbf{C}_j^H (\mathbf{F} \text{diag}(\mathbf{v}_j) \mathbf{H} + \mathbf{N}_j), \quad j \in [J], \end{aligned} \quad (12)$$

where the cascaded channel and noise matrices are respectively defined as

$$\begin{aligned} \mathbf{H} &\triangleq [\mathbf{H}_1 \quad \dots \quad \mathbf{H}_K] \in \mathbb{C}^{N \times KL} \\ \mathbf{N}_j &\triangleq [\mathbf{N}_{[j,1]} \quad \dots \quad \mathbf{N}_{[j,K]}] \in \mathbb{C}^{N \times KL}. \end{aligned}$$

*Remark 2:* Due to the use of hybrid beamforming structures, the BS can observe the  $N_{\text{RF}} \times L$  matrix during each subframe. Whereas, the  $M \times L$  matrix is observed when (conventional) fully-digital beamforming is employed. To attain the same amount of the training observations, the training overhead becomes the  $M/N_{\text{RF}}$  times bigger. Naturally, in our simulations in Section V, the scale of the training overhead tends to be larger than those in [12], [13], [39] based on fully-digital systems. ■

### IV. THE PROPOSED CHANNEL ESTIMATION METHOD

In this section, we present an efficient method to estimate the effective (or cascaded) channels  $\{\mathbf{H}_{[\text{eff},k]} : k \in [K]\}$  in (2) from the processed training observations  $\{\mathbf{Z}_j : j \in [J]\}$  in (12). As shown in Section II-B, the BS-RIS channel (i.e.,  $\mathbf{F}$ ) is expressed as the linear combination of the  $N_f$  rank-1 matrices in the both *near-* and *far-field* channels. Since the rank of  $\mathbf{F}$  (denoted by  $\text{rk}(\mathbf{F})$ ) is less than equal to  $N_f$ ,  $\mathbf{F}$  is a low-rank matrix in mmWave channels. This is one of the key ingredients for the proposed channel estimation method. Let  $\mathbf{S}_{\text{col}}$  denote the  $M \times \text{rk}(\mathbf{F})$  matrix whose columns are the basis of the column space of  $\mathbf{F}$  (a.k.a. common column space). Regardless of the channel characteristics (i.e., the near- and far-field channels) of  $\mathbf{F}$ , each effective channel  $\mathbf{H}_{[\text{eff},k,\ell]}$  in (3) can be represented as the *low-rank* decomposition:

$$\mathbf{H}_{[\text{eff},k,\ell]} = \mathbf{S}_{\text{col}} \mathbf{T}_{[k,\ell]}, \quad k \in [K], \ell \in [L], \quad (13)$$

where  $\mathbf{T}_{[k,\ell]} \in \mathbb{C}^{\text{rk}(\mathbf{F}) \times N}$  denotes a user and antenna specific coefficient matrix. On the basis of the low-rank decomposition, the proposed channel estimation method consists of the two parts (see Fig. 3). In the first part, using the training observations from the first  $M_{\text{RF}}B$  subframes, the column space of  $\mathbf{F}$  (i.e.,  $\mathbf{S}_{\text{col}}$ ) is estimated by means of a collaborative low-rank approximation. Then, using the training observations from the remaining  $NB_r$  subframes, the coefficient matrices  $\mathbf{T}_{[k,\ell]}$ 's are jointly optimized. Thus, the proposed channel estimation method is named Collaborative Low-Rank Approximation and Joint Optimization (CLRA-JO). Also, the training overhead of the proposed CLRA-JO is computed as

$$J = M_{\text{RF}}B_c + NB_r, \quad (14)$$

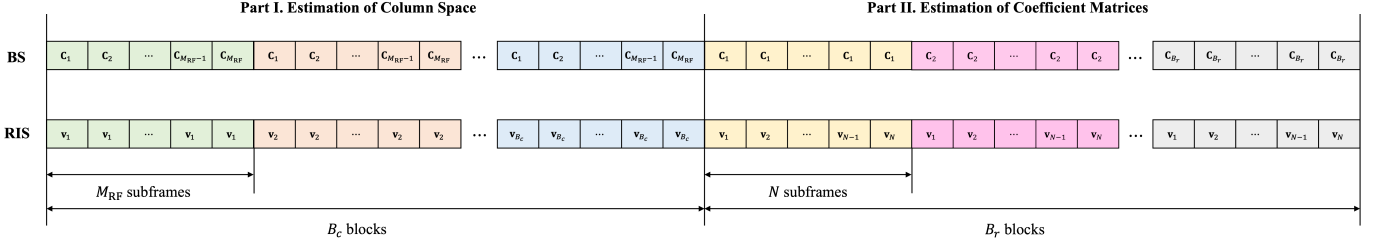


Fig. 3. The proposed channel estimation protocol and frame structure, where each subframe consists of  $T$  (i.e., the length of a pilot sequence) time slots, where  $M_{\text{RF}} = M/N_{\text{RF}}$ .

where  $B_c$  and  $B_r$  denote the hyperparameters which can control the tradeoff between the estimation accuracy and the training overhead.

In the subsequent subsections, we will design the RF combining matrices  $\{\mathbf{C}_j : j \in [J]\}$  and the reflection vectors  $\{\mathbf{v}_j : j \in [J]\}$ , in order to derive the processed observations suitable for the proposed channel estimation method. Before describing them, we provide the useful definition below:

*Definition 2:* Let  $\Phi_{[X,Y]}$  be a  $X \times Y$  matrix having orthonormal columns. In the following, we will construct the RF combining matrices and the reflection vectors using the matrix  $\Phi_{[X,Y]}$ . In practice, a DFT matrix can be adopted as the  $\Phi_{[X,Y]}$ . ■

#### A. Estimation of Column Space

In the first part of training, the total  $M_{\text{RF}}B_c$  subframes are employed to estimate  $\mathbf{S}_{\text{col}}$  (see Fig. 3). To design the RF combining matrices and the reflection vectors, the subframes are partitioned into  $B_c$  blocks each having  $M_{\text{RF}}$  subframes.

From the training observations  $\{\mathbf{Z}_j : j \in [M_{\text{RF}}B_c]\}$  in (12), we derive the observations suitable to estimate  $\mathbf{S}_{\text{col}}$  by properly designing  $\{\mathbf{C}_j, \mathbf{v}_j : j \in [M_{\text{RF}}B_c]\}$ . For the compactness of expressions, we re-index the training observations  $\{\mathbf{Z}_j : j \in [M_{\text{RF}}B_c]\}$ :

$$\mathbf{Z}_{[i,b]}^{\text{1st}} \triangleq \mathbf{Z}_{M_{\text{RF}}(b-1)+i}, \quad (15)$$

for  $i \in [M_{\text{RF}}]$  and  $b \in [B_c]$ . We design the RF combining matrices as

$$\mathbf{C}_{M_{\text{RF}}(b-1)+i} = \Phi_{[M,M]}(:, [N_{\text{RF}}(i-1) + 1 : N_{\text{RF}}i]), \quad (16)$$

for each  $i \in [M_{\text{RF}}]$  and for every  $b \in [B_c]$ . As shown in Fig. 3,  $\mathbf{C}_i$  is used at the  $i$ -th subframe of every block, namely, the subframe-dependent RF-combining matrices are employed. For each block  $b \in [B_c]$ , the  $M_{\text{RF}}$  reflection vectors are constructed as follows:

$$\mathbf{v}_{M_{\text{RF}}(b-1)+i} = \Phi_{[N,B_c]}(:, b), \quad \forall i \in [M_{\text{RF}}].$$

Focusing on the block  $b \in [B_c]$ , we will explain how to obtain the column-sampled observations to estimate  $\mathbf{S}_{\text{col}}$ . The exactly same procedures are applied to every block. Letting  $\mathbf{Q}_b \triangleq \text{diag}(\mathbf{v}_{M_{\text{RF}}(b-1)+i})\mathbf{H} = \text{diag}(\Phi_{[N,B_c]}(:, b))\mathbf{H}$  and with the above constructions, we obtain the following observations from (12):

$$\mathbf{Z}_{[i,b]}^{\text{1st}} = \mathbf{C}_{M_{\text{RF}}(b-1)+i}^{\text{H}} \mathbf{F} \mathbf{Q}_b + \tilde{\mathbf{N}}_{[i,b]}, \quad (17)$$

where  $\tilde{\mathbf{N}}_{[i,b]}$  is denoted as  $\mathbf{C}_{M_{\text{RF}}(b-1)+i}^{\text{H}} \mathbf{N}_{M_{\text{RF}}(b-1)+i}$ . For each block  $b \in [B_c]$ , we can get:

$$\begin{aligned} \tilde{\mathbf{Z}}_{[\text{col},b]} &= \Phi_{[M,M]} \begin{bmatrix} \mathbf{Z}_{[1,b]}^{\text{1st}} \\ \vdots \\ \mathbf{Z}_{[M_{\text{RF}},b]}^{\text{1st}} \end{bmatrix} \in \mathbb{C}^{M \times KL} \\ &\stackrel{(a)}{=} \Phi_{[M,M]} \Phi_{[M,M]}^{\text{H}} (\mathbf{F} \mathbf{Q}_b + \tilde{\mathbf{N}}_{[\text{col},b]}) \\ &= \mathbf{F} \mathbf{Q}_b + \tilde{\mathbf{N}}_{[\text{col},b]}, \end{aligned} \quad (18)$$

where (a) is due to the proposed RF combining matrices in (16) and

$$\tilde{\mathbf{N}}_{[\text{col},b]} = \Phi_{[M,M]} \begin{bmatrix} \tilde{\mathbf{N}}_{[1,b]} \\ \vdots \\ \tilde{\mathbf{N}}_{[M_{\text{RF}},b]} \end{bmatrix}.$$

From  $\{\tilde{\mathbf{Z}}_{[\text{col},b]} : b \in [B_c]\}$ , we can obtain the processed observations suitable for estimating  $\mathbf{S}_{\text{col}}$ :

$$\begin{aligned} \mathbf{M}_{\text{col}} &\triangleq [\tilde{\mathbf{Z}}_{[\text{col},1]} \quad \cdots \quad \tilde{\mathbf{Z}}_{[\text{col},B_c]}] \in \mathbb{C}^{M \times B_c KL} \\ &= \mathbf{F} \mathbf{Q} + \tilde{\mathbf{N}}_{\text{col}}, \end{aligned} \quad (19)$$

where  $\tilde{\mathbf{N}}_{\text{col}} \triangleq [\tilde{\mathbf{N}}_{[\text{col},1]} \quad \cdots \quad \tilde{\mathbf{N}}_{[\text{col},B_c]}]$  and  $\mathbf{Q} \triangleq [\mathbf{Q}_1 \quad \cdots \quad \mathbf{Q}_{B_c}]$ . Noticeably, since  $\mathbf{Q}$  is a full-rank matrix with high-probability (i.e.,  $\text{rank}(\mathbf{Q}) = \text{rank}(\mathbf{H}) = N$  with high-probability), the column space of  $\mathbf{M}_{\text{col}}$  can be equivalent to that of  $\mathbf{F}$ , provided that  $B$  is larger than  $\text{rk}(\mathbf{F})$  and the impact of noise is very small.

We explain how to estimate  $\mathbf{S}_{\text{col}}$  from the processed observations  $\mathbf{M}_{\text{col}}$  in (19). Recall that  $\mathbf{S}_{\text{col}}$  is the  $M \times \text{rk}(\mathbf{F})$  matrix whose columns are the basis of the column space of  $\mathbf{F}$ . To estimate it, we find the eigenvalue decomposition of the covariance matrix of  $\mathbf{M}_{\text{col}}$ :

$$\mathbf{M}_{\text{col}} \mathbf{M}_{\text{col}}^{\text{H}} = \tilde{\mathbf{S}}_{\text{col}} \Sigma_{\text{col}} \tilde{\mathbf{S}}_{\text{col}}^{\text{H}}, \quad (20)$$

where  $\tilde{\mathbf{S}}_{\text{col}}$  is the eigenvectors corresponding to the eigenvalue matrix

$$\Sigma_{\text{col}} = \text{diag}([\lambda_{[\text{col},1]}, \lambda_{[\text{col},2]}, \dots, \lambda_{[\text{col},M]}]),$$

where the eigenvalues  $\lambda_{[\text{col},\ell]}$ 's are ordered in a descending order in magnitude. As suggested in [13], the  $\text{rk}(\mathbf{F})$  (i.e., the

rank of  $\mathbf{F}$  (or  $\mathbf{S}_{\text{col}}$ ) can be efficiently estimated using the minimum description length (MDL) criterion [40] as

$$\widehat{\text{rk}}(\mathbf{F}) = \arg \min_{n \in [M]} \left\{ -\log \left( \frac{\prod_{i=n+1}^M \lambda_{[\text{col},i]}^{\frac{1}{M-n}}}{\frac{1}{M-n} \sum_{i=n+1}^M \lambda_{[\text{col},i]}} \right)^{(M-n)B_c T} + \frac{1}{2} n (2M - n) \log(B_c T) \right\}. \quad (21)$$

As long as independent columns are sufficiently sampled, the optimization below can yield a good  $\widehat{\text{rk}}(\mathbf{F})$ -dimensional column space of  $\mathbf{F}$  [41]:

$$\hat{\mathbf{S}}_{\text{col}} = \arg \min_{\mathbf{S} \in \mathbb{C}^{M \times \widehat{\text{rk}}(\mathbf{F})}, \mathbf{S}^H \mathbf{S} = \mathbf{I}} \left\| (\mathbf{I} - \mathbf{S} \mathbf{S}^H) \mathbf{M}_{\text{col}} \mathbf{M}_{\text{col}}^H \right\|_2^2. \quad (22)$$

The objective function can measure the distance between the column spaces of  $\mathbf{S}$  and  $\mathbf{M}_{\text{col}}$  since the difference of  $\mathbf{S} \mathbf{S}^H \mathbf{M}_{\text{col}}$  (i.e., the projections of the columns of  $\mathbf{M}_{\text{col}}$  onto the column space of  $\mathbf{S}$ ) and  $\mathbf{M}_{\text{col}}$  should be zero if  $\mathbf{S}$  and  $\mathbf{M}_{\text{col}}$  has the same column space. From Eckart–Young–Mirsky Theorem [42], the optimal solution to the above problem is derived as

$$\hat{\mathbf{S}}_{\text{col}} = \tilde{\mathbf{S}}_{\text{col}}(:, [\widehat{\text{rk}}(\mathbf{F})]). \quad (23)$$

As in [43], the accuracy of the estimated column space can be measured by the Euclidean distance between the BS-RIS channel (i.e.,  $\mathbf{F}$  and the BS-RIS channel projected on the estimated column space (i.e.,  $\hat{\mathbf{S}}_{\text{col}} \hat{\mathbf{S}}_{\text{col}}^H \mathbf{F}$ ). Also, its upper bound was derived as

$$\left\| (\mathbf{I} - \hat{\mathbf{S}}_{\text{col}} \hat{\mathbf{S}}_{\text{col}}^H) \mathbf{F} \right\|_F \leq \frac{\delta}{B_c K L}, \quad (24)$$

for some  $\delta > 0$ . We can obtain a *multi-user gain* since the upper bound can decrease as  $K$  grows. Namely, given a target accuracy level, we can reduce the pilot overhead  $B_c$  inversely proportional to  $K$ .

### B. Estimation of Coefficient Matrices

We propose an iterative algorithm to estimate the coefficient matrices  $\{\mathbf{T}_{[k,\ell]} : k \in [K], \ell \in [L]\}$  in (13). We first identify the some relationship among the effective channels due to their special structure in (3):

$$\begin{aligned} \mathbf{H}_{[\text{eff},k,\ell]} &= \mathbf{F} \text{diag}(\mathbf{H}_k(:, \ell)) \\ &= \mathbf{F} [\text{diag}(\mathbf{H}_1(:, 1)) \text{diag}(\mathbf{H}_1(:, 1))^{-1}] \text{diag}(\mathbf{H}_k(:, \ell)) \\ &= \mathbf{F} \text{diag}(\mathbf{H}_1(:, 1)) \mathbf{D}_{[k,\ell]} = \mathbf{H}_{[\text{eff},1,1]} \mathbf{D}_{[k,\ell]}, \end{aligned}$$

where  $\mathbf{D}_{[k,\ell]} \triangleq \text{diag}(\mathbf{H}_1(:, 1))^{-1} \text{diag}(\mathbf{H}_k(:, \ell))$  is the  $N \times N$  diagonal matrix. Since  $\mathbf{H}_{[\text{eff},1,1]} = \mathbf{S}_{\text{col}} \mathbf{T}_{[1,1]}$ , each coefficient matrix  $\mathbf{T}_{[k,\ell]}$  can be expressed as

$$\mathbf{T}_{[k,\ell]} = \mathbf{T}_{[1,1]} \mathbf{D}_{[k,\ell]}, \quad k \in [K], \ell \in [L]. \quad (25)$$

We thus need to estimate the  $\mathbf{T}_{[1,1]}$  and the diagonal matrices  $\{\mathbf{D}_{[k,\ell]} : k \in [K], \ell \in [L]\}$ . To design RF combining matrices and reflection vectors, the subframes in the second part are partitioned into  $B_r$  blocks each having  $N$  subframes (see Fig. 3). For simplicity, we let  $n_0 \triangleq M_{\text{RF}} B$  denote the index of the last subframe in the first part. From the training observations  $\{\mathbf{Z}_j : j \in [n_0 + 1 : J]\}$  in (12),

we derive the processed observations suitable to estimate the  $\mathbf{T}_{[1,1]}$  and  $\{\mathbf{D}_{[k,\ell]} : k \in [K], \ell \in [L]\}$  by properly designing  $\{\mathbf{C}_j, \mathbf{V}_j : j \in [n_0 + 1 : J]\}$ . As before, we re-index the training observations  $\{\mathbf{Z}_j : j \in [n_0 + 1 : J]\}$  such as

$$\mathbf{Z}_{[i,b]}^{2\text{nd}} \triangleq \mathbf{Z}_{n_0 + M_{\text{RF}}(b-1) + i}, \quad b \in [B_r], i \in [N]. \quad (26)$$

For each  $b \in [B_r]$  and for every  $i \in [N]$ , we design the RF combining matrices  $\mathbf{C}_{n_0 + M_{\text{RF}}(b-1) + i}$  as

$$\Phi_{[M, N_{\text{RF}} B_r]}(:, [N_{\text{RF}}(b-1) + 1 : N_{\text{RF}} b]). \quad (27)$$

For each  $i \in [N]$  and for every  $b \in [B_r]$ , the reflection vector is constructed as

$$\mathbf{v}_{n_0 + M_{\text{RF}}(b-1) + i} = \Phi_{[N, N]}(:, i). \quad (28)$$

With the above constructions and from (12) and (26), we can define an user- and antenna-wise observation:

$$\begin{aligned} \mathbf{Z}_{[i,b,k,\ell]}^{2\text{nd}} &\triangleq \mathbf{Z}_{[i,b]}^{2\text{nd}}(:, L(k-1) + \ell) \\ &\stackrel{(a)}{=} \mathbf{C}_{n_0 + M_{\text{RF}}(b-1) + i}^H \mathbf{H}_{[\text{eff},k,\ell]} \Phi_{[N, N]}(:, i) + \tilde{\mathbf{N}}_{[i,b,k,\ell]}, \end{aligned}$$

where (a) follows from (3), (11), and (28), and where

$$\tilde{\mathbf{N}}_{[i,b,k,\ell]} = \mathbf{C}_{n_0 + M_{\text{RF}}(b-1) + i}^H \mathbf{N}_{n_0 + M_{\text{RF}}(b-1) + i}(:, L(k-1) + \ell).$$

For each block  $b \in [B_r]$ , we can get:

$$\begin{aligned} \bar{\mathbf{Z}}_{[b,k,\ell]} &\triangleq \begin{bmatrix} \mathbf{Z}_{[1,b,k,\ell]}^{2\text{nd}} & \cdots & \mathbf{Z}_{[N,b,k,\ell]}^{2\text{nd}} \end{bmatrix} \Phi_{[N, N]}^H \\ &= \mathbf{C}_{n_0 + M_{\text{RF}}(b-1) + i}^H \mathbf{H}_{[\text{eff},k,\ell]} \Phi_{[N, N]} \Phi_{[N, N]}^H + \tilde{\mathbf{N}}_{[b,k,\ell]} \\ &= \mathbf{C}_{n_0 + M_{\text{RF}}(b-1) + i}^H \mathbf{H}_{[\text{eff},k,\ell]} + \tilde{\mathbf{N}}_{[b,k,\ell]}, \end{aligned}$$

where

$$\tilde{\mathbf{N}}_{[b,k,\ell]} = \begin{bmatrix} \tilde{\mathbf{N}}_{[1,b,k,\ell]} & \cdots & \tilde{\mathbf{N}}_{[N,b,k,\ell]} \end{bmatrix} \Phi_{[N, N]}^H.$$

Stacking  $\{\bar{\mathbf{Z}}_{[b,k,\ell]} : b \in [B_r]\}$ , we define:

$$\begin{aligned} \mathbf{M}_{[\text{row},k,\ell]} &\triangleq \begin{bmatrix} \bar{\mathbf{Z}}_{[1,k,\ell]} \\ \vdots \\ \bar{\mathbf{Z}}_{[B_r,k,\ell]} \end{bmatrix} \in \mathbb{C}^{N_{\text{RF}} B_r \times N} \\ &\stackrel{(a)}{=} \Phi_{[M, N_{\text{RF}} B_r]}^H \mathbf{H}_{[\text{eff},k,\ell]} + \tilde{\mathbf{N}}_{[\text{row},k,\ell]} \\ &\stackrel{(b)}{=} \Phi_{[M, N_{\text{RF}} B_r]}^H \mathbf{S}_{\text{col}} \mathbf{T}_{[k,\ell]} + \tilde{\mathbf{N}}_{[\text{row},k,\ell]}, \end{aligned} \quad (29)$$

where (a) is due to the proposed RF combining matrices in (27), (b) is from the decomposition in (13), and

$$\tilde{\mathbf{N}}_{[\text{row},k,\ell]} \triangleq \begin{bmatrix} \tilde{\mathbf{N}}_{[1,k,\ell]} \\ \vdots \\ \tilde{\mathbf{N}}_{[B_r,k,\ell]} \end{bmatrix}.$$

Letting  $\mathbf{P} \triangleq \Phi_{[M, N_{\text{RF}} B_r]}^H \hat{\mathbf{S}}_{\text{col}} \in \mathbb{C}^{N_{\text{RF}} B_r \times \widehat{\text{rk}}(\mathbf{F})}$ , we directly derive the solution of the individual least-square (LS) estimation using the pseudo-inverse  $\mathbf{P}^\dagger$ :

$$\begin{aligned} \hat{\mathbf{T}}_{[k,\ell]}^{\text{LS}} &\triangleq \mathbf{P}^\dagger \mathbf{M}_{[\text{row},k,\ell]} \in \mathbb{C}^{\widehat{\text{rk}}(\mathbf{F}) \times N} \\ &= \mathbf{P}^\dagger \left( \Phi_{[M, N_{\text{RF}} B_r]}^H \mathbf{H}_{[\text{eff},k,\ell]} + \tilde{\mathbf{N}}_{[\text{row},k,\ell]} \right) \\ &= \mathbf{P}^\dagger \left( \Phi_{[M, N_{\text{RF}} B_r]}^H \mathbf{S}_{\text{col}} \mathbf{T}_{[k,\ell]} + \tilde{\mathbf{N}}_{[\text{row},k,\ell]} \right). \end{aligned} \quad (30)$$

Here, the existence of the  $\mathbf{P}^\dagger$  can be guaranteed by choosing the hyperparameter  $B_r$  such that

$$N_{\text{RF}} B_r \geq \widehat{\text{rk}}(\mathbf{F}). \quad (31)$$

Normally, we have  $B_r = 1$  for very sparse channel, i.e.,  $N_{\text{RF}} \geq \widehat{\text{rk}}(\mathbf{F})$ .

The LS solutions would be good in very high SNRs. Whereas, it is well-known that the multiplication of the pseudo-inverse would increase the power of the noise vector  $\tilde{\mathbf{N}}_{[\text{row},k,\ell]}$ , which can degrade the performance in practical SNRs. Thus, there is a room to enhance the estimation accuracy harnessing the property in (25).

$$\begin{aligned} & \arg \min_{\mathbf{T}_{[1,1]}, \mathbf{D}_{[1,1]}, \dots, \mathbf{D}_{[K,L]}} \mathcal{L}(\mathbf{T}_{[1,1]}, \{\mathbf{D}_{[k,\ell]}\}) \\ & \text{subject to } \mathbf{D}_{[k,\ell]} \text{ s are diagonal matrices,} \end{aligned} \quad (32)$$

where

$$\mathcal{L}(\mathbf{T}_{[1,1]}, \{\mathbf{D}_{[k,\ell]}\}) \triangleq \sum_{k=1}^K \sum_{\ell=1}^L \left\| \hat{\mathbf{T}}_{[k,\ell]}^{\text{LS}} - \mathbf{T}_{[1,1]} \mathbf{D}_{[k,\ell]} \right\|_F^2.$$

We efficiently solve this problem via an alternating optimization (see Algorithm 1).

**Iterations.** At the  $t$ -th iteration, the proposed alternating optimization is performed as follows:

- For the fixed  $\hat{\mathbf{T}}_{[1,1]}^{(t-1)}$ , our optimization can be formulated as

$$\begin{aligned} \hat{\mathbf{D}}_{[k,\ell]}^{(t)} &= \arg \min_{\mathbf{D}_{[k,\ell]}} \mathcal{L} \left( \hat{\mathbf{T}}_{[1,1]}^{(t-1)}, \mathbf{D}_{[k,\ell]} \middle| \hat{\mathbf{T}}_{[1,1]}^{(t-1)} \right) \\ &= \arg \min_{\mathbf{D}_{[k,\ell]}} \left\| \hat{\mathbf{T}}_{[k,\ell]}^{\text{LS}} - \hat{\mathbf{T}}_{[1,1]}^{(t-1)} \mathbf{D}_{[k,\ell]} \right\|_F^2, \end{aligned} \quad (33)$$

for  $k \in [K]$ ,  $\ell \in [L]$ , where the initial value is determined as  $\hat{\mathbf{T}}_{[1,1]}^{(0)} = \hat{\mathbf{T}}_{[1,1]}^{\text{LS}}$ . This LS problem is easily solved as

$$\hat{\mathbf{D}}_{[k,\ell]}^{(t)} = \text{diag} \left( \mathbf{R}(:, \Omega_N)^\dagger \hat{\mathbf{t}}_{[k,\ell]}^{\text{LS}}(\Omega_N) \right), \quad (34)$$

where  $\mathbf{R} = \mathbf{I} \otimes \hat{\mathbf{T}}_{[1,1]}^{(t-1)} \in \mathbb{C}^{N_f N \times N^2}$  and  $\Omega_N = \{n + (n-1)N : n \in [N]\}$ . Also, vectorization of  $\hat{\mathbf{T}}_{[k,\ell]}^{\text{LS}}$  is denoted as  $\hat{\mathbf{t}}_{[k,\ell]}^{\text{LS}} = \text{vec}(\hat{\mathbf{T}}_{[k,\ell]}^{\text{LS}}) \in \mathbb{C}^{\widehat{\text{rk}}(\mathbf{F})N \times 1}$ .

- For the fixed  $\{\hat{\mathbf{D}}_{[k,\ell]}^{(t)} : k \in [K], \ell \in [L]\}$ , our optimization can be formulated as a standard LS problem:

$$\begin{aligned} \hat{\mathbf{T}}_{[1,1]}^{(t)} &= \arg \min_{\mathbf{T}} \mathcal{L} \left( \mathbf{T}, \{\hat{\mathbf{D}}_{[k,\ell]}^{(t)}\} \middle| \{\hat{\mathbf{D}}_{[k,\ell]}^{(t)}\} \right) \\ &= \arg \min_{\mathbf{T}} \sum_{k=1}^K \sum_{\ell=1}^L \left\| \hat{\mathbf{T}}_{[k,\ell]}^{\text{LS}} - \mathbf{T} \hat{\mathbf{D}}_{[k,\ell]}^{(t)} \right\|_F^2, \end{aligned} \quad (35)$$

where  $\hat{\mathbf{D}}_{[1,1]}^{(t)} = \mathbf{I}$  during iterations. The optimal solution is derived as

$$\begin{aligned} \hat{\mathbf{T}}_{[1,1]}^{(t)} &= \left( \sum_{k=1}^K \sum_{\ell=1}^L \hat{\mathbf{T}}_{[k,\ell]}^{\text{LS}} \left( \hat{\mathbf{D}}_{[k,\ell]}^{(t)} \right)^{\text{H}} \right) \\ &\quad \times \left( \sum_{k=1}^K \sum_{\ell=1}^L \hat{\mathbf{D}}_{[k,\ell]}^{(t)} \left( \hat{\mathbf{D}}_{[k,\ell]}^{(t)} \right)^{\text{H}} \right)^{-1}. \end{aligned} \quad (36)$$

After the  $t_{\text{max}}$  iterations, the estimated cascaded effective channels are given by

$$\hat{\mathbf{H}}_{[\text{eff},k,\ell]} = \hat{\mathbf{S}}_{\text{col}} \hat{\mathbf{T}}_{[1,1]}^{(t_{\text{max}})} \hat{\mathbf{D}}_{[k,\ell]}^{(t_{\text{max}})}. \quad (37)$$

---

### Algorithm 1 Proposed CLRA-JO Algorithm

---

- 1: **Input:**  $\hat{\mathbf{S}}_{\text{col}}$  (i.e., the estimated column space of  $\mathbf{F}$ ) in (23),  $\{\mathbf{M}_{[\text{row},k,\ell]} : k \in [K], \ell \in [L]\}$  in (29), and the maximum number of iterations  $t_{\text{max}}$ .
- 2: **Initialization:** Set  $\hat{\mathbf{T}}_{[1,1]}^{(0)} = \hat{\mathbf{T}}_{[1,1]}^{\text{LS}}$  from (30).
- 3: **Repeat until**  $t = t_{\text{max}}$ 
  - Given  $\hat{\mathbf{T}}_{[1,1]}^{(t-1)}$ , update the  $\hat{\mathbf{D}}_{[k,\ell]}^{(t)}$  via (34).
  - Given  $\{\hat{\mathbf{D}}_{[k,\ell]}^{(t)} : k \in [K], \ell \in [L]\}$ , update  $\hat{\mathbf{T}}_{[1,1]}^{(t)}$  via (36).
- 4: **Output:** The estimated RIS-aided effective channels:

$$\hat{\mathbf{H}}_{[\text{eff},k,\ell]} = \hat{\mathbf{S}}_{\text{col}} \hat{\mathbf{T}}_{[1,1]}^{(t_{\text{max}})} \hat{\mathbf{D}}_{[k,\ell]}^{(t_{\text{max}})}.$$


---

### C. Analysis

In this section, we analyze the convergence and the computational complexity of the proposed channel estimation method.

1) *Convergence Analysis:* We prove the convergence of the proposed iterative algorithm in Algorithm 1. Toward this, we show that

$$\mathcal{L} \left( \hat{\mathbf{T}}_{[1,1]}^{(t-1)}, \{\hat{\mathbf{D}}_{[k,\ell]}^{(t-1)}\} \right) \geq \mathcal{L} \left( \hat{\mathbf{T}}_{[1,1]}^{(t)}, \{\hat{\mathbf{D}}_{[k,\ell]}^{(t)}\} \right). \quad (38)$$

This implies that as  $t$  grows, the  $\hat{\mathbf{T}}_{[1,1]}^{(t)}$  and  $\{\hat{\mathbf{D}}_{[k,\ell]}^{(t)}\}$  converge to the optimal solution of our optimization in (32). Specifically, the proof is provided as follows:

$$\begin{aligned} \mathcal{L} \left( \hat{\mathbf{T}}_{[1,1]}^{(t-1)}, \{\hat{\mathbf{D}}_{[k,\ell]}^{(t-1)}\} \right) &= \mathcal{L} \left( \hat{\mathbf{T}}_{[1,1]}^{(t-1)}, \{\hat{\mathbf{D}}_{[k,\ell]}^{(t-1)}\} \middle| \hat{\mathbf{T}}_{[1,1]}^{(t-1)} \right) \\ &\stackrel{(a)}{\geq} \min_{\{\mathbf{D}_{[k,\ell]}^{(t-1)}\}} \mathcal{L} \left( \hat{\mathbf{T}}_{[1,1]}^{(t-1)}, \{\mathbf{D}_{[k,\ell]}^{(t-1)}\} \middle| \hat{\mathbf{T}}_{[1,1]}^{(t-1)} \right) \\ &\stackrel{(b)}{=} \mathcal{L} \left( \hat{\mathbf{T}}_{[1,1]}^{(t-1)}, \{\hat{\mathbf{D}}_{[k,\ell]}^{(t)}\} \middle| \hat{\mathbf{T}}_{[1,1]}^{(t-1)} \right) \\ &= \mathcal{L} \left( \hat{\mathbf{T}}_{[1,1]}^{(t-1)}, \{\hat{\mathbf{D}}_{[k,\ell]}^{(t)}\} \right) = \mathcal{L} \left( \hat{\mathbf{T}}_{[1,1]}^{(t-1)}, \{\hat{\mathbf{D}}_{[k,\ell]}^{(t)}\} \middle| \{\hat{\mathbf{D}}_{[k,\ell]}^{(t)}\} \right) \\ &\stackrel{(c)}{\geq} \min_{\mathbf{T}_{[1,1]}} \mathcal{L} \left( \mathbf{T}_{[1,1]}, \{\hat{\mathbf{D}}_{[k,\ell]}^{(t)}\} \middle| \{\hat{\mathbf{D}}_{[k,\ell]}^{(t)}\} \right) \\ &\stackrel{(d)}{=} \mathcal{L} \left( \hat{\mathbf{T}}_{[1,1]}^{(t)}, \{\hat{\mathbf{D}}_{[k,\ell]}^{(t)}\} \middle| \{\hat{\mathbf{D}}_{[k,\ell]}^{(t)}\} \right) = \mathcal{L} \left( \hat{\mathbf{T}}_{[1,1]}^{(t)}, \{\hat{\mathbf{D}}_{[k,\ell]}^{(t)}\} \right), \end{aligned}$$

where (a) holds with equality when  $\{\hat{\mathbf{D}}_{[k,\ell]}^{(t-1)}\}$  are optimum, (b) follows from the fact that each of  $\{\hat{\mathbf{D}}_{[k,\ell]}^{(t)}\}$  is the optimal solution of the minimization in (33), (c) holds with equality when  $\hat{\mathbf{T}}_{[1,1]}^{(t-1)}$  is optimum, and (d) is due to the fact that  $\hat{\mathbf{T}}_{[1,1]}^{(t)}$  is the optimal solution of the minimization in (35).

2) *Complexity Analysis:* We derive the computational complexity of the proposed channel estimation method. Following the related work in [13], we measure the computational complexity by counting the number of complex multiplication (CM). Regarding the complexity of the estimation of column



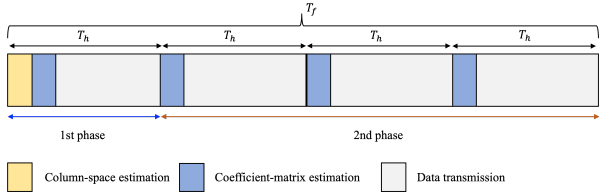


Fig. 4. The description of two-phase communication protocol.

space in (22), we need to perform the eigenvalue decomposition, which requires  $\mathcal{O}(M^3)$  computational complexity. Also, the dominant complexity of the proposed joint optimization in Algorithm 1 comes from the computations in (30), (34) and (36), which respectively require

$$\Delta_{LS} \triangleq N \left( \widehat{\text{rk}}(\mathbf{F}) \right)^2 KL \quad (39)$$

$$\Delta_D \triangleq N(3\widehat{\text{rk}}(\mathbf{F}) + 1)KL \quad (40)$$

$$\Delta_T \triangleq N(\widehat{\text{rk}}(\mathbf{F}) + 2)KL. \quad (41)$$

Thus, the overall computational complexity of the proposed CLRA-JO is computed as

$$\Psi_{\text{CLRA-JO}} = \mathcal{O}(M^3 + \Delta_{LS} + t_{\max}(\Delta_D + \Delta_T)). \quad (42)$$

*Remark 3:* The proposed channel estimation method can be efficiently operated under the two-phase communication protocol in Fig. 4. The key idea is based on the fact that the coherence time of the BS-RIS channel (denoted by  $T_f$ ) is commonly much longer than that of the RIS-User channels (denoted by  $T_h$ ). Accordingly,  $\mathbf{S}_{\text{col}}$  and  $\mathbf{T}_{[k,\ell]}$ 's are changed every  $T_f$  and  $T_h$  time slots, respectively. Following this protocol, the overall training overhead becomes lower as  $T_f$  grows. Namely, in the second phase, we only require the  $NB_r$  training overhead, instead of  $M_{\text{RF}}B_c + NB_r$ . In our simulations in Section V, the effectiveness of the two-phase communication protocol will be demonstrated. Moreover, the two-phase communication protocol can reduce the computational complexity in (42) since in this case, the impact of the complexity  $\mathcal{O}(M^3)$  can be negligible. ■

## V. SIMULATION RESULTS

In this section, we evaluate the performances of the proposed channel estimation method for RIS-aided mmWave MU-MIMO systems with hybrid beamforming structures. Regarding the wireless channels in our simulations, we consider the XL-RIS assisted XL-MIMO and RIS-aided massive MIMO systems, defined in Section II-B. In Section V-A, we demonstrate the superiority of the proposed CLRA-JO for XL-RIS assisted XL-MIMO systems by comparing with the state-of-the-art (SOTA) CS-based methods in [13]. Remarkably, for the first time, we take into account the near-field BS-RIS and near-field RIS-User channels (in short, near-near field channel). In Section V-B, we then verify the practicality of the proposed CLRA-JO via experiments on *real* 28GHz UPA channel data in [44]. Following the performance metric in the related works [12], [13], [28], [29], we employ the normalized

mean square error (NMSE) for the evaluation of channel estimation accuracy, given by

$$\text{NMSE} \triangleq \mathbb{E} \left[ \frac{1}{K} \sum_{k=1}^K \frac{\|\hat{\mathbf{H}}_{[\text{eff},k]} - \mathbf{H}_{[\text{eff},k]}\|_F^2}{\|\mathbf{H}_{[\text{eff},k]}\|_F^2} \right]. \quad (43)$$

The expectation is evaluated by Monte Carlo simulations with  $10^3$  trials.

### A. XL-RIS Assisted XL-MIMO Systems

In this section, we verify the superiority of the proposed channel estimation method (named CLRA-JO) for XL-RIS assisted XL-MIMO systems, by evaluating its performances in the following categories of wireless channels:

- Far-far field channels: Both  $\mathbf{F}$  and  $\{\mathbf{H}_k : k \in [K]\}$  are all far-field channels. Note that this case is identical to the RIS-aided massive MIMO channel.
- Far-near field channels:  $\mathbf{F}$  is a far-field channel and  $\{\mathbf{H}_k : k \in [K]\}$  are all near-field channels.
- Near-near field channels: Both  $\mathbf{F}$  and  $\{\mathbf{H}_k : k \in [K]\}$  are all near-field channels.

For our simulations, we consider the MU-MIMO system with  $M = N = 16 \times 8 = 128$ ,  $L = 2 \times 2 = 4$ ,  $N_{\text{RF}} = 8$ , the number of spatial paths  $N_f = N_{h_k} = 3$ ,  $\forall k \in [K]$ , the system frequency  $f = 50$  GHz, and the wavelength  $\lambda = c/f = 0.006\text{m}$ . According to the system wavelength  $\lambda$ , the RD and MIMO-RD are respectively computed as

$$Z_{\text{RD}} = 49.152\text{m} \text{ and } Z_{\text{MRD}} = 196.608\text{m}.$$

The distance between the BS and the RIS are chosen as  $z_f = 250\text{m}$  and  $z_r = 150\text{m}$  to build the far- and near-field channels, respectively. Also, the distances between the RIS and the  $K$  users (denoted by  $\{z_{h_k} : k \in [K]\}$ ) are uniformly distributed over  $[60\text{m}, 70\text{m}]$  and  $[20\text{m}, 30\text{m}]$  to form the far- and near-field channels, respectively. The signal-to-noise ratio (SNR) is defined as

$$\text{SNR} = 10 \log \left( \frac{P}{\sigma^2} \right) [\text{dB}], \quad (44)$$

where  $P$  and  $\sigma^2$  are defined in (9) and (10), respectively. Specifically, we set that  $\sigma^2 = 1$  and  $P$  is described as a relative value of the noise power. Regarding the modeling of wireless channels, the power is equally divided into each signal path, the  $i$ -th normalized complex channel gains of  $\{\mathbf{H}_k : k \in [K]\}$  and  $\mathbf{F}$  are respectively determined as

$$\alpha_{h_k}^i = \sqrt{\frac{NL}{N_{h_k}}} \psi_{h_k}^i \text{ and } \alpha_f^i = \sqrt{\frac{MN}{N_f}} \psi_f^i, \quad (45)$$

where  $\psi_{h_k}^i$  and  $\psi_f^i$  are chosen uniformly from  $[0, \pi]$ . The angle of all AoDs and AoAs are chosen uniformly and randomly from  $[0, \pi]$ .

For comparison, the following benchmark methods are considered:

- **CLRA-LS:** In the proposed CLRA-JO, the coefficient matrices can be simply obtained from the LS estimation (i.e.,  $\hat{\mathbf{T}}_k^{\text{LS}}$  in (30)) instead of the joint optimization in Algorithm 1, this simplified method is referred to as

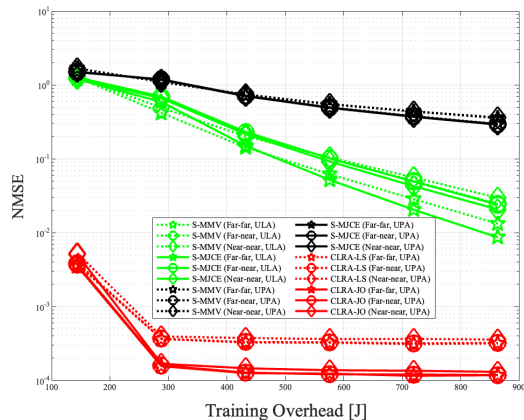


Fig. 5. The impact of the training overhead on the NMSE. SNR = 0 dB and  $K = 4$ .

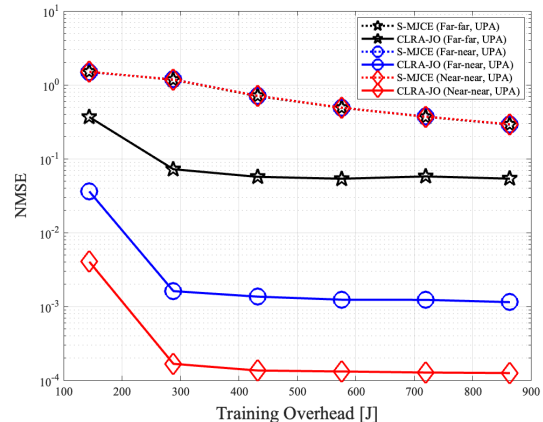


Fig. 7. The impact of the training overhead and distance on the NMSE.  $K = 4$ .

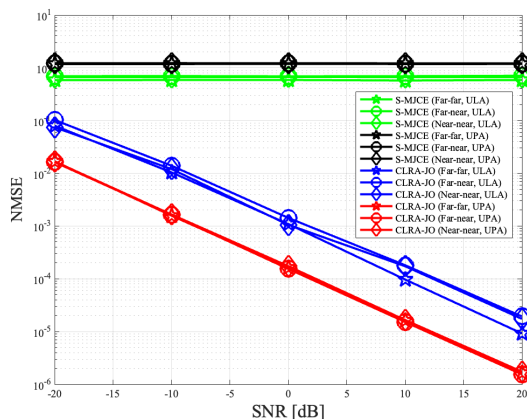


Fig. 6. The impact of SNR on the NMSE.  $K = 4$  and  $B_c = 10$ .

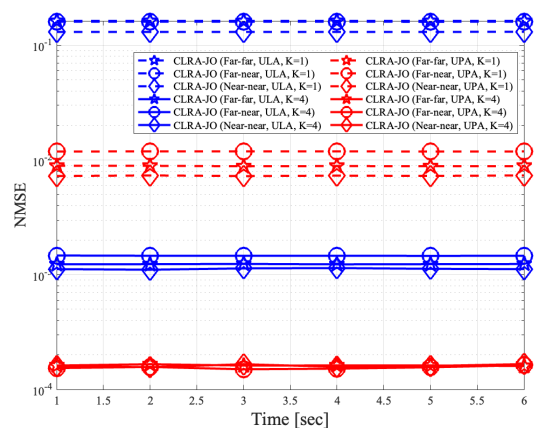


Fig. 8. The impact of the proposed two-phase communication protocol on the NMSE. SNR = 0 dB and  $B_c = 10$ .

CLRA-LS. This method is considered to identify the performance gain of the joint optimization.

- **S-MMV**: The channels are estimated by projecting the received signals onto the common column space first, and solved by formulating a multiple measurements vector (MMV) Problem. Here, the MMV problem is addressed via SOMP algorithm. (see Algorithm 1 in [13]).
- **S-MJCE**: The channels are estimated by the two-step (subspace) multi-user joint channel estimation procedure. (see Algorithm 2 in [13]). This method is considered as the best-known CS-based method.

In the benchmark CS methods, the resolution of the quantization for the dictionary are set by  $G = 512$ . Also, in the proposed CLRA-JO, we choose the  $B_r = 1$  and  $t_{\max} = 10$  in Algorithm 1.

*Remark 4*: In the existing *near-field* channel estimation methods in [17], [20], [31], [32], it is assumed that the number of spatial paths for the BS-RIS and RIS-User channels (denoted by  $N_f$  and  $\{N_{h_k} : k \in [K]\}$ , respectively) are exactly known a priori. This makes the existing methods impractical. Also, ULA was only considered since it is quite challenging to design a dictionary representing *near-field* UPA

array response vectors or solve a 2D-ANM problem in a large system. Thus, they cannot be employed in our system model based on practical UPA and their extension to UPA is non-trivial. Because of this, the CS-based method in [13] was adopted as the benchmark method, wherein UPA dictionaries for both far- and near-field channels are designed by means of the Kronecker product of the horizontal ULA dictionary and the vertical ULA dictionary. This is the common way to design an UPA dictionary [13], [38]. ■

Fig. 5 shows the impact of training overhead on the NMSE. We observe that the proposed CLRA-based methods can outperform the existing CS-based methods in all the training overhead and all the categories of wireless channels. Comparing the performances of CLRA-JO and CLRA-LS, we can verify the effectiveness of the proposed joint optimization in Section IV-B. Remarkably, the proposed CLRA-JO can attain higher channel estimation accuracy than the SOTA CS-based methods while reducing the pilot overhead about 80% (i.e.,  $J = 144$  and  $J = 864$  for CLRA-based and CS-based methods, respectively). We also observe that the proposed CLRA-JO shows the almost similar performances regardless of

the categories of wireless channels, which verifies that CLRA-JO is indeed the unified method. The CS-based methods perform worse in practical UPA than ULA since they suffer from the severe grid-mismatch problem.

Fig. 6 shows the impact of SNR on the NMSE. We first observe that in all the categories of wireless channels, the performances of CLRA-JO improve as SNR grows. On the other hand, the performances of the CS-based methods are saturated due to the inevitable grid-mismatch problem. Namely, the saturation level is determined according to the quantization resolution of steering vectors. Together with the results in Fig. 5, it is confirmed that the proposed CLRA-JO is more suitable for practical UPA than the CS-based methods.

Fig. 7 shows the impact of training overhead and physical distances on the NMSE. Regarding the BS-RIS and RIS-User channels, the distance-dependent large-scale path loss parameters are given as  $PL(z) = 10^{-2}z^{-2.2}$  [45]. While the distribution of the near-near channel and noise remains as in Fig. 5, the channel gains of the far-far and far-near channels are set by the near-near channel and  $PL(z)$ . We observe that the proposed method can better performance in the near-near channel than the far-near and far-far channels. This is because, in the near-near channel, the SNR gain of the received signals can be obtained as the physical distance of this channel is shorter than those in the other two channels. Obviously, it is a natural result to be obtained if a channel estimation method is well-developed. In contrast, the CS-based methods cannot attain any estimation gain in terms of distance.

Fig. 8 shows the impact of the proposed two-phase communication protocol in Fig. 4 on the NMSE. In this simulation, the coherence times are set by  $T_f = 6$  sec and  $T_{h_k} = 1$  sec,  $\forall k \in [K]$ . As expected, the column space estimated only in the first phase (i.e., during the first 1 sec) can be effectively reused for channel estimations in the remaining second phase. Thus, as aforementioned, this protocol can reduce the computational complexity as well as the training overhead. Under the two-phase communication protocol, the proposed CLRA-JO requires about 2.8% computational complexity of S-MMV (i.e., the CS-based method having the lowest computational complexity). Here, the computational complexity of the S-MMV is provided in [13] such as

$$\Psi_{\text{S-MMV}} = \mathcal{O}\left(M^3 + N^2(\widehat{\text{rk}}(\mathbf{F})KL + G)\right).$$

We also note that the proposed CLRA-JO can indeed yield the multi-user gain since the performance with  $K = 4$  outperforms that with  $K = 1$ . The performance gain is attained since the accuracy of the common column space estimation and the proposed joint optimization are improved as the  $K$  grows.

Based on the above analysis, we can conclude that the proposed CLRA-JO would be a good practical candidate as the channel estimation method for XL-RIS assisted multi-user XL-MIMO.

### B. RIS-Aided Massive MIMO Systems: 28GHz Channel Data

In this section, we demonstrate the effectiveness of the proposed CLRA-JO for the massive MIMO systems with  $M = N = 8 \times 8 = 64$ ,  $L = 2 \times 2 = 4$ , and  $N_{\text{RF}} = 8$ . In the

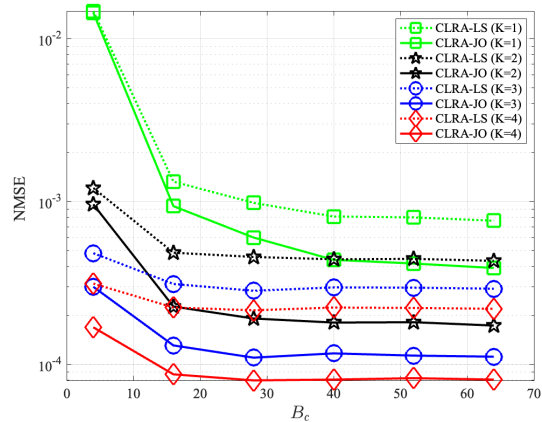


Fig. 9. The impact of  $B_c$  and  $K$  on the NMSE. SNR = 0 dB,  $N_f = 3$  and  $N_{h_k} = 3$ ,  $\forall k \in [K]$ .

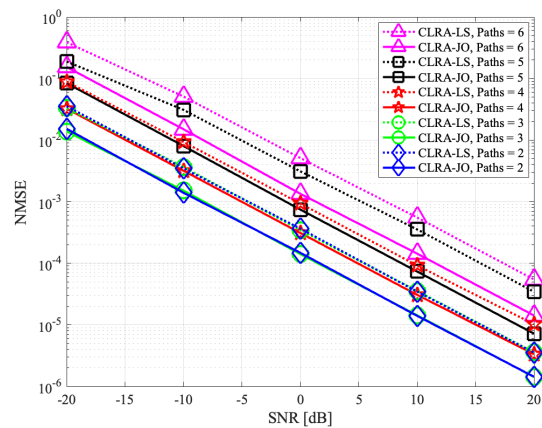


Fig. 10. The impact of SNR and  $N_f$  on the NMSE:  $K = 4$ ,  $B_c = 10$  and  $N_{h_k} = 4 \forall k \in [K]$ .

proposed method, we choose the  $B_r = 1$  and  $t_{\text{max}} = 10$  in Algorithm 1. Also, the *real* 28GHz UPA channels are considered, in which the experimental data in [44] is used. Regarding the distances among the BS, RIS, and  $K$  users,  $z_f = 50\text{m}$  and  $\{z_{h_k} : k \in [K]\}$  are uniformly distributed over  $[5\text{m}, 10\text{m}]$ . Also, the distance-dependent path loss  $PL(z)$  ( $z = z_f$  or  $z = z_{h_k}$ ) is modeled as

$$PL(z) [\text{dB}] = \alpha + 10\beta \log_{10}(z) + \epsilon, \quad (46)$$

where  $\epsilon \sim \mathcal{N}(0, \nu^2)$ . Here, the channel parameters in (46) are set by  $\alpha = 61.4$ ,  $\beta = 2$ , and  $\nu = 5.8$  dB for the line-of-sight (LOS) paths, and  $\alpha = 72.0$ ,  $\beta = 2.92$ , and  $\nu = 8.7$  dB for the non-line-of-sight (NLOS) paths. From these parameters, the complex channel gains of  $\{\mathbf{H}_k : k \in [K]\}$  and  $\mathbf{F}$  are independently distributed according to  $\mathcal{CN}(0, \gamma_{h_k}^2 10^{-0.1PL(z_{h_k})})$  and  $\mathcal{CN}(0, \gamma_f^2 10^{-0.1PL(z_f)})$ , respectively, where the normalization factor is determined as  $\gamma_{h_k} = \sqrt{NL/N_{h_k}}$  and  $\gamma_f = \sqrt{MN/N_f}$ . In this real experimental data, the SNR defined in (44) is defined with

$$\sigma^2 = 10^{-0.1(PL(z_{h_k}) + PL(z_f))}. \quad (47)$$

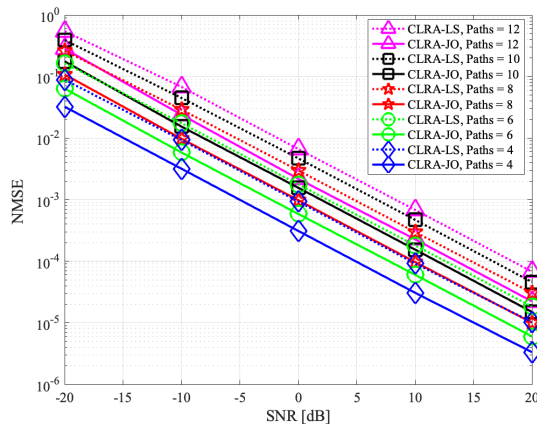


Fig. 11. The impact of SNR and  $N_{h_k}$ , denoted by Paths in label, on the NMSE:  $K = 4$ ,  $B_c = 10$  and  $N_f = 4$

Fig. 9 shows the impact of training overhead  $B_c$  and the number of users  $K$  on the NMSE. From the comparisons with CLRA-LS, we can verify that our joint optimization in (32) indeed enhances the estimation accuracy of the user-specific coefficient matrices. We can see that the accuracy of the estimated  $\mathbf{S}_{\text{col}}$  gets better as the number of users  $K$  grows. Remarkably, when the number of users is large (i.e.,  $K \geq 3$ ), the proposed channel estimation method can achieve an attractive performance with a very small training overhead. Thus, in practical MU-MIMO systems, the proposed method is very promising by considerably reducing the pilot overhead.

Figs. 10 and 11 show the impact of SNR and the number of signal paths on the NMSE. As expected, the estimation accuracy is enhanced as SNR increases (i.e., the noise perturbation in (30) becomes less). From the comparison with CLRA-LS, we can verify the effectiveness of the proposed joint optimization in Section IV-B, by alleviating the effect of lower SNR. Specifically, our joint optimization can attain the about SNR = 5 dB gain compared with CLRA-LS. As expected, the estimation accuracy improves as  $N_f$  and  $N_{h_k}$  decrease. Thus, the proposed method is well-suited to the next-generation mmWave or THz communication systems, where the corresponding wireless channels consist of lower scattering and a smaller number of signal paths.

## VI. CONCLUSION

We studied the channel estimation problem for XL-RIS assisted multi-user XL-MIMO systems with hybrid beamforming structures. In this system, we proposed the unified channel estimation method (named CLRA-JO) which can perform in the far- and near-field channels without any modification. Whereas, in the existing CS-based methods, dictionary should be designed by taking into account the characteristics of the near- and far-field channels. Via simulations and complexity analysis, it is demonstrated that the proposed CLRA-JO can yield better estimation accuracy than the state-of-the-art CS-based methods while having lower training overhead (e.g., the 80% reduction of the pilot overhead). Our on-going work is to design channel state information (CSI) feedback suitable

for the proposed CLRA JO so that it can be applicable in frequency-division-duplexing (FDD)-based XL-RIS assisted multi-user XL-MIMO systems.

## REFERENCES

- [1] M. Di Renzo, A. Zappone, M. Debbah, M.-S. Alouini, C. Yuen, J. De Rosny, and S. Tretyakov, "Smart radio environments empowered by reconfigurable intelligent surfaces: How it works, state of research, and the road ahead," *IEEE journal on selected areas in communications*, vol. 38, no. 11, pp. 2450–2525, 2020.
- [2] X. Pei, H. Yin, L. Tan, L. Cao, Z. Li, K. Wang, K. Zhang, and E. Björnson, "Ris-aided wireless communications: Prototyping, adaptive beamforming, and indoor/outdoor field trials," *IEEE Transactions on Communications*, vol. 69, no. 12, pp. 8627–8640, 2021.
- [3] Q. Wu, S. Zhang, B. Zheng, C. You, and R. Zhang, "Intelligent reflecting surface-aided wireless communications: A tutorial," *IEEE transactions on communications*, vol. 69, no. 5, pp. 3313–3351, 2021.
- [4] R. Long, Y.-C. Liang, Y. Pei, and E. G. Larsson, "Active intelligent reflecting surface for simo communications," in *IEEE Global Communications Conference*. IEEE, 2020, pp. 1–6.
- [5] G. Zhou, C. Pan, H. Ren, K. Wang, M. Di Renzo, and A. Nallanathan, "Robust beamforming design for intelligent reflecting surface aided mimo communication systems," *IEEE Wireless Communications Letters*, vol. 9, no. 10, pp. 1658–1662, 2020.
- [6] G. Zhou, C. Pan, H. Ren, K. Wang, M. El-kashlan, and M. Di Renzo, "Stochastic learning-based robust beamforming design for ris-aided millimeter-wave systems in the presence of random blockages," *IEEE Transactions on Vehicular Technology*, vol. 70, no. 1, pp. 1057–1061, 2021.
- [7] Q. Wu and R. Zhang, "Intelligent reflecting surface enhanced wireless network via joint active and passive beamforming," *IEEE transactions on wireless communications*, vol. 18, no. 11, pp. 5394–5409, 2019.
- [8] C. Liao, F. Wang, and V. K. Lau, "Optimized design for irs-assisted integrated sensing and communication systems in clutter environments," *IEEE Transactions on Communications*, 2023.
- [9] M. Z. Win, Z. Wang, Z. Liu, Y. Shen, and A. Conti, "Location awareness via intelligent surfaces: A path toward holographic nln," *IEEE Vehicular Technology Magazine*, vol. 17, no. 2, pp. 37–45, 2022.
- [10] Z. Wang, Z. Liu, Y. Shen, A. Conti, and M. Z. Win, "Location awareness in beyond 5g networks via reconfigurable intelligent surfaces," *IEEE Journal on Selected Areas in Communications*, vol. 40, no. 7, pp. 2011–2025, 2022.
- [11] H. Wymeersch, J. He, B. Denis, A. Clemente, and M. Juntti, "Radio localization and mapping with reconfigurable intelligent surfaces: Challenges, opportunities, and research directions," *IEEE Vehicular Technology Magazine*, vol. 15, no. 4, pp. 52–61, 2020.
- [12] C.-R. Tsai, Y.-H. Liu, and A.-Y. Wu, "Efficient compressive channel estimation for millimeter-wave large-scale antenna systems," *IEEE Transactions on Signal Processing*, vol. 66, no. 9, pp. 2414–2428, 2018.
- [13] J. Chen, Y.-C. Liang, H. V. Cheng, and W. Yu, "Channel estimation for reconfigurable intelligent surface aided multi-user mmwave mimo systems," *IEEE Transactions on Wireless Communications*, no. 10, pp. 6853–6869, 2023.
- [14] Y. Chi, L. L. Scharf, A. Pezeshki, and A. R. Calderbank, "Sensitivity to basis mismatch in compressed sensing," *IEEE Transactions on Signal Processing*, vol. 59, no. 5, pp. 2182–2195, 2011.
- [15] L. Wei, C. Huang, G. C. Alexandropoulos, C. Yuen, Z. Zhang, and M. Debbah, "Channel estimation for ris-empowered multi-user mimo wireless communications," *IEEE Transactions on Communications*, vol. 69, no. 6, pp. 4144–4157, 2021.
- [16] Y. Guo, P. Sun, Z. Yuan, C. Huang, Q. Guo, Z. Wang, and C. Yuen, "Efficient channel estimation for ris-aided mimo communications with unitary approximate message passing," *IEEE Transactions on Wireless Communications*, vol. 22, no. 2, pp. 1403–1416, 2022.
- [17] M. Cui and L. Dai, "Channel estimation for extremely large-scale mimo: Far-field or near-field?" *IEEE Transactions on Communications*, vol. 70, no. 4, pp. 2663–2677, 2022.
- [18] W. Liu, C. Pan, H. Ren, F. Shu, S. Jin, and J. Wang, "Low-overhead beam training scheme for extremely large-scale ris in near field," *IEEE Transactions on Communications*, 2023.
- [19] T. S. Rappaport, Y. Xing, O. Kanhere, S. Ju, A. Madanayake, S. Mandal, A. Alkhateeb, and G. C. Trichopoulos, "Wireless communications and applications above 100 ghz: Opportunities and challenges for 6g and beyond," *IEEE Access*, vol. 7, pp. 78 729–78 757, 2019.

- [20] Y. Lu and L. Dai, "Near-field channel estimation in mixed los/nlos environments for extremely large-scale mimo systems," *IEEE Transactions on Communications*, vol. 71, no. 6, pp. 3694–3707, 2023.
- [21] C. Lin and G. Y. L. Li, "Terahertz communications: An array-of-subarrays solution," *IEEE Communications Magazine*, vol. 54, no. 12, pp. 124–131, 2016.
- [22] A. F. Molisch, V. V. Ratnam, S. Han, Z. Li, S. L. H. Nguyen, L. Li, and K. Haneda, "Hybrid beamforming for massive mimo: A survey," *IEEE Communications magazine*, vol. 55, no. 9, pp. 134–141, 2017.
- [23] P. Wang, J. Fang, L. Dai, and H. Li, "Joint transceiver and large intelligent surface design for massive mimo mmwave systems," *IEEE transactions on wireless communications*, vol. 20, no. 2, pp. 1052–1064, 2020.
- [24] I. Yildirim, A. Koc, E. Basar, and T. Le-Ngoc, "Ris-aided angular-based hybrid beamforming design in mmwave massive mimo systems," in *GLOBECOM 2022-2022 IEEE Global Communications Conference*. IEEE, 2022, pp. 5267–5272.
- [25] S. H. Hong, J. Park, S.-J. Kim, and J. Choi, "Hybrid beamforming for intelligent reflecting surface aided millimeter wave mimo systems," *IEEE Transactions on Wireless Communications*, vol. 21, no. 9, pp. 7343–7357, 2022.
- [26] R. Schroeder, J. He, and M. Juntti, "Channel estimation for hybrid ris aided mimo communications via atomic norm minimization," in *2022 IEEE International Conference on Communications Workshops (ICC Workshops)*. IEEE, 2022, pp. 1219–1224.
- [27] H. Chung and S. Kim, "Location-aware beam training and multi-dimensional anm-based channel estimation for ris-aided mmwave systems," *IEEE Transactions on Wireless Communications*, vol. 23, no. 1, pp. 652,666, 2023.
- [28] J. Lee and S. Hong, "Channel estimation for ris-aided mmwave mu-mimo systems: Collaborative low-rank matrix completion approach," in *IEEE International conference on Network Intelligence and Digital Content (IC-NIDC)*. IEEE, 2024, pp. 1–5.
- [29] H. Chung, S. Hong, and S. Kim, "Efficient multi-user channel estimation for ris-aided mmwave systems using shared channel subspace," *IEEE Transactions on Wireless Communications*, 2024.
- [30] T. Hastie, R. Mazumder, J. D. Lee, and R. Zadeh, "Matrix completion and low-rank svd via fast alternating least squares," *The Journal of Machine Learning Research*, vol. 16, no. 1, pp. 3367–3402, 2015.
- [31] S. Yang, W. Lyu, Z. Hu, Z. Zhang, and C. Yuen, "Channel estimation for near-field xl-ris-aided mmwave hybrid beamforming architectures," *IEEE Transactions on Vehicular Technology*, vol. 72, no. 8, pp. 11 029–11 034, 2023.
- [32] X. Yu, W. Shen, R. Zhang, C. Xing, and T. Q. S. Quek, "Channel estimation for xl-ris-aided millimeter-wave systems," *IEEE Transactions on Communications*, vol. 71, no. 9, pp. 5519–5533, 2023.
- [33] I. Ahmed, H. Khammari, A. Shahid, A. Musa, K. S. Kim, E. De Poorter, and I. Moerman, "A survey on hybrid beamforming techniques in 5g: Architecture and system model perspectives," *IEEE Communications Surveys & Tutorials*, vol. 20, no. 4, pp. 3060–3097, 2018.
- [34] R. Li, B. Guo, M. Tao, Y.-F. Liu, and W. Yu, "Joint design of hybrid beamforming and reflection coefficients in ris-aided mmwave mimo systems," *IEEE Transactions on Communications*, vol. 70, no. 4, pp. 2404–2416, 2022.
- [35] Q. Wu and R. Zhang, "Beamforming optimization for wireless network aided by intelligent reflecting surface with discrete phase shifts," *IEEE Transactions on Communications*, vol. 68, no. 3, pp. 1838–1851, 2020.
- [36] S. Moon, H. Lee, J. Choi, and Y. Lee, "Low-complexity beamforming optimization for irs-aided mu-mimo wireless systems," *IEEE Transactions on Vehicular Technology*, vol. 71, no. 5, pp. 5587–5592, 2022.
- [37] J. Lee and S. Hong, "Asymptotically near-optimal hybrid beamforming for mmwave irs-aided mimo systems," *arXiv preprint arXiv:2403.09083*, 2024.
- [38] F. Zheng, "Extremely large-scale array systems: Near-filed codebook design and performance analysis," *arXiv preprint arXiv:2306.01458*, 2023.
- [39] C. Hu, L. Dai, S. Han, and X. Wang, "Two-timescale channel estimation for reconfigurable intelligent surface aided wireless communications," *IEEE Transactions on Communications*, vol. 69, no. 11, pp. 7736–7747, 2021.
- [40] M. Wax and T. Kailath, "Detection of signals by information theoretic criteria," *IEEE Transactions on acoustics, speech, and signal processing*, vol. 33, no. 2, pp. 387–392, 1985.
- [41] J. Chae, P. Narayanamurthy, S. Bac, S. M. Sharada, and U. Mitra, "Column-based matrix approximation with quasi-polynomial structure," in *ICASSP 2023-2023 IEEE International Conference on Acoustics, Speech and Signal Processing (ICASSP)*. IEEE, 2023, pp. 1–5.
- [42] C. Eckart and G. Young, "The approximation of one matrix by another of lower rank," *Psychometrika*, vol. 1, no. 3, pp. 211–218, 1936.
- [43] M. Xu, R. Jin, and Z.-H. Zhou, "Cur algorithm for partially observed matrices," in *International Conference on Machine Learning*. PMLR, 2015, pp. 1412–1421.
- [44] M. R. Akdeniz, Y. Liu, M. K. Samimi, S. Sun, S. Rangan, T. S. Rappaport, and E. Erkip, "Millimeter wave channel modeling and cellular capacity evaluation," *IEEE Journal on Selected Areas in Communications*, vol. 32, no. 6, pp. 1164–1179, 2014.
- [45] V. Raghavan, L. Akhondzadeh-Asl, V. Podshivalov, J. Hulten, M. A. Tassoudji, O. H. Koymen, A. Sampath, and J. Li, "Statistical blockage modeling and robustness of beamforming in millimeter-wave systems," *IEEE Transactions on Microwave Theory and Techniques*, vol. 67, no. 7, pp. 3010–3024, 2019.